Robust coupling of superconducting order parameter in a mesoscale NbN-Fe-NbN epitaxial structure

S. K. Bose and R. C. Budhani[*]

Condensed Matter - Low Dimensional Systems Laboratory, Department of Physics,

Indian Institute of Technology Kanpur, Kanpur - 208016, India

(Dated: July 9, 2009)

Abstract

We report an unconventional and promising route to self-assemble distributed superconductor-ferromagnet-superconductor (S-F-S) Josephson Junctions on single crystal [100] MgO. These structures consist of [110] epitaxial nano-plaquettes of Fe covered with superconducting NbN films of varying thickness. The S-F-S structures are characterized by a strong magnetoresistance (MR) anisotropy for the in-plane and out-of-plane magnetic fields. The stronger in-plane MR suggests decoherence of S-F-S junctions whose critical current follows a $(1 - T/T_c)$ and $(1 - T/T_c)^{1/2}$ dependence for $T \approx T_c$ and $T \ll T_c$ respectively, in accordance with the theory of supercurrent transport in such junctions.

PACS numbers: 74.81.Cp, 75.75.+a, 74.50.+r

---
[*]Electronic address: rcb@iitk.ac.in

The tunneling of Cooper pair order parameter through a thin barrier separating two bulk superconductors, as predicted by Josephson[1] and seen subsequently in thin film junctions[2] has had a far reaching impact on physics and technology. The applications of Josephson Junctions (JJs) range from sensors for ultralow magnetic fields and weak electromagnetic radiation[3], millimeter wave resonators[4], programmable voltage standards[5], superconducting flux qubits[6], etc. The physics of JJs changes remarkably when the barrier material is a ferromagnet[7, 8]. Interesting effects with rich underlying physics and many promising applications are expected in superconductor-ferromagnet (S-F) hybrids of nanoscale dimensions[9]. In recent years nanoscale S-F structures have been synthesized using the conventional approaches of nano-lithography such as electron beam patterning, atomic force microscopy, and focused ion beam milling.

In this letter we report observation of a giant anisotropic magnetoresistance (MR) in self-assembled nanometer-scale-distributed junctions of Fe and superconducting NbN. Our methodology of synthesis utilizes stress-tuned Volmer-Weber (VW) type[10] plaquette growth of Fe on [100] MgO, whose electrical connectivity is tuned by NbN layers of different thickness (d_{NbN}) deposited on top of the VW template. A KrF excimer laser (λ =248 nm) based pulsed laser ablation technique was used to deposit the nanostructured Fe and epitaxial NbN thin films as described in our earlier works[11, 12]. In brief, the growth and the post-growth annealing temperature for Fe plaquettes was $\sim$700 °C whereas the NbN layer was deposited at 200 °C to inhibit the formation of iron nitride at NbN-Fe interfaces. The nominal thickness of the Fe base layer is 40 nm, whereas d_{NbN} =10, 20, and 30 nm have been used.

The scanning electron micrographs (SEM) of the samples as shown in Fig. 1(a & b) reveal that the Fe template consists of nearly perfect square plaquettes of $\approx$100 $\times$ 100 nm^2
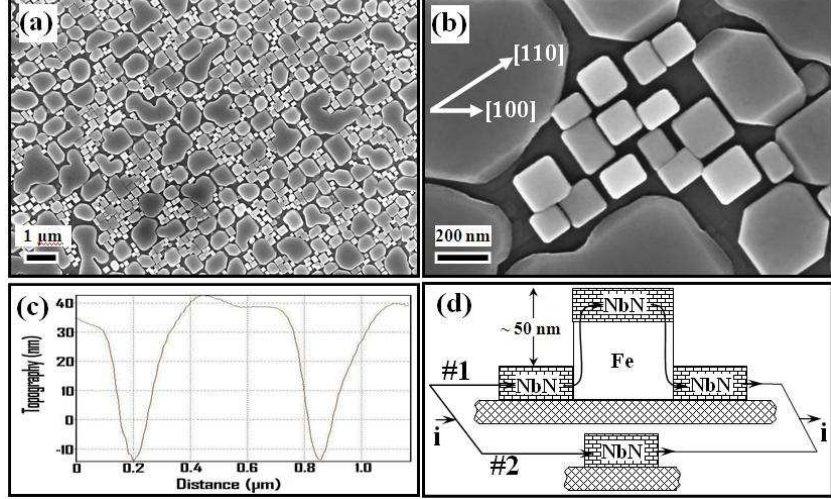
FIG. 1: (a & b) Scanning electron micrographs of the Fe(40 nm) / NbN(30 nm) sample. The top of nearly perfect square Fe plaquettes and the inter-plaquette space is covered with epitaxial NbN. (c) A typical atomic-force-microscope line scan showing the height of Fe plaquettes. (d) A sketch showing the two distinct parallel paths for the flow of supercurrent through the S-F-S hybrid. Path ♯1 is for the NbN-Fe-NbN junctions and ♯2 for current flow through the percolating backbone of NbN.

area, separated by ≈20 nm gaps and are aligned along MgO [110] direction. The NbN grows epitaxially on the plaquettes and the inter-plaquette gaps. This has been confirmed with x-ray diffraction and x-ray fluorescence mapping of niobium. A typical atomic force microscope (AFM) line scan shown in Fig. 1(c) reveals that the requirement of mass conservation makes the Fe nano-plaquettes thicker than the programmed thickness of ≈40 nm. Due to this unique structure, the flow of supercurrent in this S-F hybrid occurs through two parallel channels as shown in Fig. 1(d). One of these paths (i.e. ♯1) is the double S-F-S junction, in which supercurrent goes vertically up through thin Fe layers into the intra-plaquette NbN and then comes down, again through the Fe. The other route (♯2) is the thin percolating backbone of NbN in the inter-plaquette spaces. As will be shown later, the path ♯1 involving
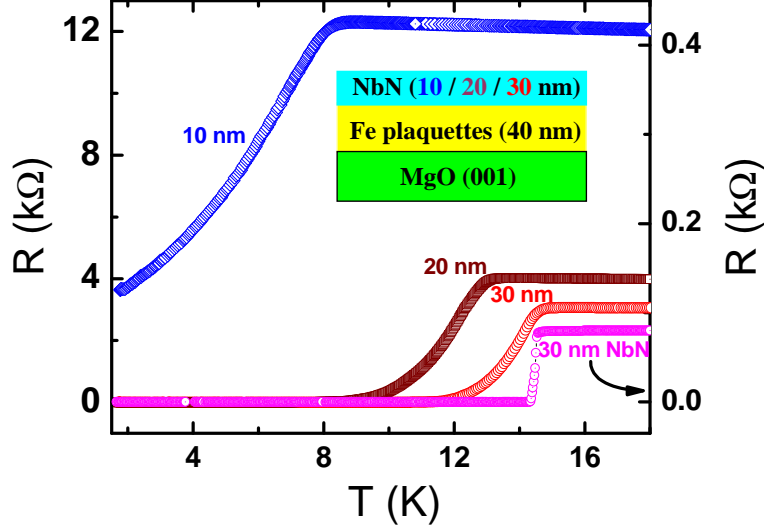
3

FIG. 2: (Color online) The temperature dependence of resistance of the 10, 20 , 30 nm NbN covered Fe plaquettes (left Y-scale) and 30 nm thick pure NbN film (right Y-scale). The onset temperature of superconductivity (T_{onset}) for 30 nm hybrid is the same as of plane 30 nm NbN film, whereas the T_c and ΔT_c are affected significantly when the NbN cover layer thickness is reduced.

double S-F-S junctions is of greater significance for supercurrent transport in these hybrids.

Fig. 2 shows the superconducting (SC) transition measured across bridges of $\approx 75 \times 1300$ μm^2 area, created by Ar^+ ion milling of the S-F hybrids. For comparison the SC-transition of a plane 30 nm thick NbN film is also shown in Fig. 2. A significant drop in transition temperature (T_c) and increase in the width of the transition (ΔT_c) along with a gain in the normal state resistance (R_n) is seen as d_{NbN} is reduced from 30 to 10 nm. In fact, the T_c drops nearly twice as fast for the hybrid ($\approx 49\%$) in comparison to the drop seen in a plane NbN film ($\approx 24\%$)[13] as the film thickness d_{NbN} is reduced from 30 to 10 nm. The R_n increases with decrease in temperature, but remains lower than the quantum resistance for Cooper pairs ($R_Q = h/4e^2 \sim 6.4$ k$\Omega/\square$), above which a superconductor-insulator transition is seen in granular films[14]. We also notice that although the R_n of the hybrid with 30 nm
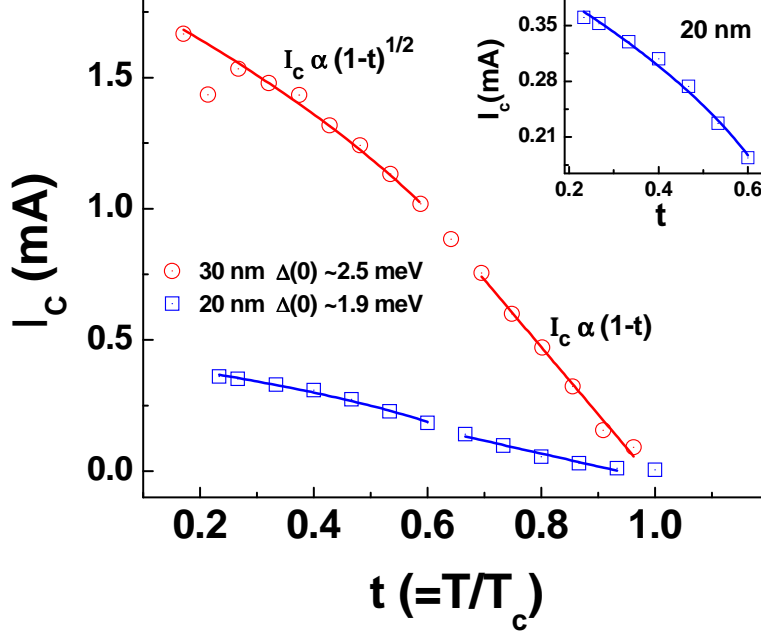
FIG. 3: (Color online) Critical current (I_c) variation with temperature for the 30 and 20 nm NbN covered Fe plaquettes. Two distinct regimes of temperature dependence can be seen in the figure. At $t > 0.7$ it goes as $\sim$ $(1\text{-}t)$ and for $t < 0.6$ the dependence is of the type $(1\text{-}t)^{1/2}$. Inset shows the $(1\text{-}t)^{1/2}$ dependence of the 20 nm NbN sample over an expanded scale.

thick NbN is three orders of magnitude higher compared to the R_n of pure NbN film, the onset temperature of superconductivity (T_{onset} $\approx$14.7 K) remains nearly the same in the two cases. The ΔT_c ($\approx$2 K) of this hybrid, however is seven times higher than of pure NbN ($\approx$0.3 K). This observation suggests that superconductivity in inter-plaquette epitaxial NbN sets in at $\approx$14.7 K, but the realization of the zero-resistance state depends on the strength and phase factor of the supercurrent through the double S-F junctions and the narrow constrictions of the epitaxial NbN backbone as sketched in Fig. 1(d).

In Fig. 3 we show the critical current (I_c) of two films (d_{NbN} $\approx$20 & 30 nm) in the $t(=T/T_c)$ range of 0.2 to 1.0. The I_c of a proximity coupled S-N-S junction depends on the number of Andreev bound states (ABS) in the normal metal (N) spacer. If the spacer is a

ferromagnet, then the spectrum of ABS is affected by the extent of exchange splitting of its conduction band[15]. It has been shown that as long as the ferromagnet thickness $d_F \ll \xi_F$, the coherance length in F layer, defined as $\xi_F = \sqrt{\hbar D/I}$, where D is the diffusion coefficient and I the exchange splitting of the ferromagnet, the maximum current (I_c) through the junctions is given as[7];

$$I_c(T) = \frac{32\sqrt{2}(\Delta/e)}{R_N} \; F(\Delta/T) \; \text{y} \; \exp(-\text{y}) \sin(\text{y}+\pi/4) \tag{1}$$

where,

$$\text{y} = \frac{d_F}{\xi_F} \left(\frac{2I}{\pi T_c} \right)^{1/2}$$

Here, $F(\Delta/T)$ has limiting values of $\frac{\pi}{128}\left(\Delta/T_c\right)$ for $T \approx T_c$ and 0.071 for $T \ll T_c$. For a given d_F and a BCS temperature dependence of the gap parameter $\Delta(T) \simeq 3.2 k_B T_c \sqrt{1-t}$, we get $I_c(T) \sim (1-t)$ for $T \approx T_c$ and $\sim \sqrt{1-t}$ for $T \ll T_c$. This temperature dependence of I_c is similar to that predicted by Ambegaokar and Baratoff for weakly coupled granular superconductors provided the suppression of gap parameter by supercurrent is not significant[16, 17]. The data in Fig. 3 have been fitted with the $(1-t)$ and $\sqrt{1-t}$ dependence for $1.0 \gtrsim t \gtrsim 0.7$ and $0.6 \gtrsim t \gtrsim 0.2$, respectively. This dependence of I_c (t) fits well over the entire temperature range and leads to $\Delta(0)$ values of 2.5 meV for 30 nm and 1.9 meV for 20 nm case respectively, which matches well with the BCS energy gap [$2\Delta(0) = 3.5 k_B T_c$] values of 2.2 meV (30 nm) and 1.93 meV (20 nm). To further point out the quality of fit, the inset shows the magnified version of $\sqrt{1-t}$ dependence of I_c for the 20 nm case.

In order to address the magnetic field (H) dependence of the coupling between the NbN layers, we investigate the state of the magnetization (M) of the Fe plaquettes. In Fig. 4 we show the M-H plots taken at 5 K, with H applied along in-plane ($H_{\parallel}$) and out-of-plane ($H_{\perp}$) direction. The out-of-plane M-H shows that the moment of Fe plaquettes is in the plane of
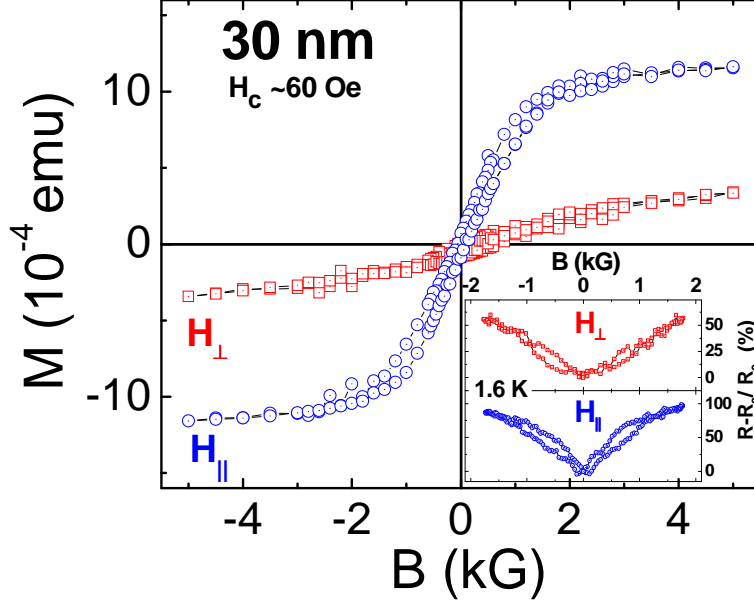
FIG. 4: (Color online) Magnetization of the 30 nm NbN covered Fe plaquettes measured at 5 K with in-plane ($H_\parallel$) and out-of-plane ($H_\perp$) fields. Inset shows the magnetoresistance measured at 1.6 K. The positive MR is twice as large for the $H_\parallel$, which is distinctly different from the behavior of a plane superconducting film where one sees a much stronger effect of $H_\perp$.

the film in agreement with the earlier studies[18].

The in-plane anisotropy of magnetization as shown in Fig. 4 affects Josephson coupling in the S-F-S junctions significantly as seen through measurements of MR, carried out at currents exceeding the critical current (I_c). While details of the angular dependence of MR will be presented elsewhere, in the inset of Fig. 4 we show the MR measured at 1.6 K as a function of applied field strength. It is clear from the figure that the positive MR at a peak field of 1500 Oe is higher by a factor of two when the field is in the plane of the film. This is a very striking result in view of the fact that for thin superconducting films it is the out-of-plane field which contributes significantly to MR, due to a copious motion of Abrikosov vortices, which is unlikely to be arrested by a possible weak pinning

7

by the inhomogeneous magnetization of Fe plaquettes. A stronger response to the $H_\parallel$ seen here is consistent with the fact that the phase of the tunneling order parameter is affected significantly when the field is in the plane of the junctions. We also note that the MR for $H_\parallel$ shows two distinct cusps at ±113 Oe, whose position is higher than the coercive field ($H_c \sim 60$ Oe) as measured by SQUID at 5 K. This observation can be understood in the context of number of magnetic entities actually taking part in the magnetization reversal process. Magnetization measurement reflects the total average response of all the magnetic plaquettes, whereas in MR the transport current samples only a fraction of the magnetic plaquettes which fall on its path[11].

In summary, we have provided a unique approach for fabrication of distributed S-F Josephson-Junctions of nanometer length scale. Our self-assembled NbN-Fe-NbN hybrids on [100] MgO shows $\approx 100\%$ MR for $H_\parallel$ which is higher by a factor of two as compared to the MR for $H_\perp$. This large in-plane response suggests breaking of phase coherence in S-F-S junctions by the planar field. Temperature dependence of supercurrent in these self-assembled structures is consistent with the theory of supercurrent transport in S-F-S junctions.

---

[1] B. D. Josephson, Phys. Lett. **1**, 251 (1962).

[2] P. W. Anderson, and J. M. Rowell, Phys. Rev. Lett. **10**, 230 (1963).

[3] S. Krey, O. Brügmann, and M. Schilling, Appl. Phys. Lett. **74**, 293 (1999).

[4] A. M. Klushin, M. He, S. L. Yan, and N. Klein, Appl. Phys. Lett. **89**, 232505 (2006).

[5] H. Schulze, R. Behr, F. Müeller, and J. Niemeyer, Appl. Phys. Lett. **73**, 996 (1998).

[6] I. Chiorescu, Y. Nakamura, C. J. P. M. Harmans, and J. E. Mooij, Science **299**, 1869 (2003).

[7] A. I. Buzdin, and M. Yu. Kupriyanov, Pis'ma Zh. Eksp. Teor. Fiz. **53**, 308 (1991) [JETP Lett. **53**, 321 (1991)].

[8] V. V. Ryazanov, V. A. Oboznov, A. Yu. Rusanov, A. V. Veretennikov, A. A. Golubov, and J. Aarts, Phys. Rev. Lett. **86**, 2427 (2001).

[9] Yuriy Makhlin, Gerd Scöhn, and Alexander Shnirman, Nature **398**, 305 (1999).

[10] S. M. Jordan, R. Schad, A. M. Keen, M. Bischoff, D. S. Schmool, and H. van Kempen, Phys. Rev. B **59**, 7350 (1999).

[11] S. K. Bose, R. Sharma, and R. C. Budhani, Phys. Rev. B **78**, 115403 (2008).

[12] K. Senapati, N. K. Pandey, Rupali Nagar, and R. C. Budhani, Phys. Rev. B **74**, 104514 (2006).

[13] S. K. Bose, and R. C. Budhani, Unpublished results.

[14] A. F. Hebard and M. A. Paalanen, Phys. Rev. Lett. **65**, 927 (1990); Ali Yazdani and Aharon Kapitulnik, Phys. Rev. Lett. **74**, 3037 (1995).

[15] T. Kontos, M. Aprili, J. Lesueur, F. Genêt, B. Stephanidis, and R. Boursier, Phys. Rev. Lett. **89**, 137007 (2002).

[16] John R. Clem, B. Bumble, S. I. Raider, W. J. Gallagher, and Y. C. Shih, Phys. Rev. B **35**, 6637 (1987).

[17] Vinay Ambegaokar and Alexis Baratoff, Phys. Rev. Lett. **10**, 486 (1963).

[18] Yongsup Park, S. Adenwalla, G. P. Felcher, and S. D. Bader, Phys. Rev. B **52**, 12779 (1995).